Superconductivity and physical properties of MgB_2

The discovery of superconductivity at 39 K in MgB_2 immediately raised the question if such a relatively high critical temperature could result from the conventional electron-phonon coupling or whether more exotic mechanisms are involved like in the copper-oxide high T_c superconductors.

In order to answer this question we calculated the electronic structure, the phonon spectrum, and the electron-phonon (e-ph) interaction using the linear-response theory within the full-potential LMTO density functional method (Phys. Rev. B **64**, 020501(R) (2001)). The crystal structure of MgB_2 is hexagonal with graphitelike boron layers stacked on top with Mg in between.

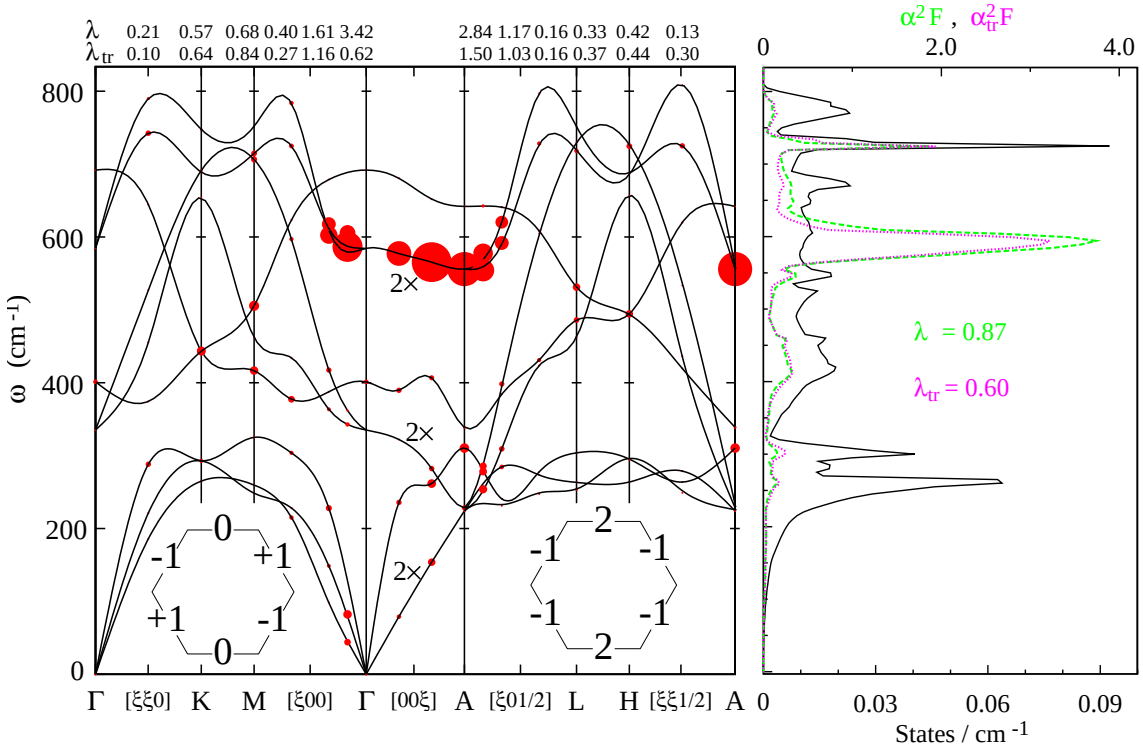

Figure 1: *Left: Calculated phonon dispersion curves in MgB_2. The area of a circle is proportional to the contribution to the electron-phonon coupling constant, λ. The insets at the bottom show the two ΓA E eigenvectors (un-normalized), which apply to the holes at the top of the σ-bands (bond-orbital coefficients) as well as to the optical bond-stretching phonons (relative change of bond lengths). Right: $F(\omega)$ (black and bottom scale), $\alpha^2(\omega)F(\omega)$ (green) and $\alpha^2_{tr}(\omega)F(\omega)$ (purple).*

The electronic structure near and below the Fermi level consists of two B p_z π-bands and three quasi-2D B-B bonding σ-bands. The σ and π bands do not hybridize when k_z=0 and π/c. The π-bands lie lower with respect to the σ-bands than in graphite and have more k_z-dispersion due to the influence of Mg, the on-top stacking, and the smaller c/a-ratio. This causes the presence of $p_{\sigma l}$=0.056 light and $p_{\sigma h}$=0.117 heavy holes near the doubly-degenerate top along ΓA of the σ-bands. For the density of states at $\varepsilon_F \equiv 0$, we find: $N(0) =$

$N_{\sigma l}(0) + N_{\sigma h}(0) + N_{\pi}(0) = 0.048 + 0.102 + 0.205 = 0.355$ states/(MgB_2·eV·spin). Along ΓA there is a doubly-degenerate σ band of symmetry E which is slightly above the Fermi level and its eigenvectors are given in the two inserts at the bottom of Fig. 1. The corresponding Fermi-surface sheets are warped cylinders.

The phonon dispersions $\omega_m(\mathbf{q})$ and density of states $F(\omega)$ are shown in Fig.1. The agreement between our $F(\omega)$ and those obtained from inelastic neutron scattering is excellent; our peaks at 260 and 730 cm^{-1} (32 and 90 meV) are seen in the experiments at 32 and 88 meV. For the frequencies of the optical Γ-modes we get: 335 cm^{-1} (E_{1u}), 401 cm^{-1} (A_{2u}), 585 cm^{-1} (E_{2g}), and 692 cm^{-1} (B_{1g}). The all-important E_{2g} modes are doubly degenerate optical B-B bond-stretching modes (obs). Close to ΓA, they have exactly the same symmetry and similar dispersions as the light and heavy σ-holes, although with the opposite signs. The E eigenfunctions shown at the bottom of Fig.1 now refer to displacement patterns, *e.g.*, $\{-1,0,1\}$ has one bond shortened, another bond stretched by the same amount, and the third bond unchanged. These E displacement patterns will obviously modulate the electronic bond energy, such as to split the light- and heavy-hole bands. It was judged that the corresponding electron-phonon (e-ph) matrix element, $g_{\sigma,obs}$, will be the dominating one.

We then calculated the e-ph interaction which is represented by the Eliashberg spectral function $\alpha^2(\omega)F(\omega)$ which for superconductivity as well as for transport is shown in the right panel of Fig.1. The dominance of the σ-σ coupling via the optical bond-stretching mode is clearly seen in the left panel of the figure, where the area of a red circle is proportional to the contribution to the electron-phonon coupling constant from the particular mode. This gives rise to the huge peak in the two Eliashberg functions around ω_{obs} = 590 cm^{-1} = 73 meV. The total $\lambda=\lambda_\sigma+\lambda_\pi$ = 0.62 + 0.25 = 0.87 is moderately large.

We first assumed isotropic pairing and obtained a T_c of 40 K by solving the Eliashberg equations for μ^* =0.10 which is at the low end of what is found for simple *sp* metals.

The temperature dependence of the specific dc resistivity calculated with the standard Bloch-Grüneisen expression is nearly isotropic and in accord with recent measurements on dense wires over the entire temperature range from 40 to 300 K.

We finally solved the Eliashberg equations for a number of temperatures from 0 K to above T_c for a fixed μ^* in the superconducting as well as in the normal state. From this we calculate the difference in specific heat in the two states which is compared to our original measurements and to some more recent measurements on high quality samples in Fig.2 (J. Phys.: Condens. Matter **14**, 1353 (2002)). It may be seen that in the calculations the specific heat jump is considerably larger at T_c than in the experiments and also that the experiments show larger heat capacity at low temperatures.

We therefore relaxed the assumption of an isotropic one band model and instead considered a two band model with the possibility of different gaps on the σ and π Fermi surface sheets (Phys. Rev. Lett. **87**, 087005 (2001)). The reason for discarding this model originally was the experimental fact that a two orders of magnitude change in scattering rate changed T_c by merely ∼2 K. With interband scattering and a two band model T_c would change much more. However, if the interband scattering is small and only intraband scattering is responsible for the change in scattering rate then a small change of T_c would be possible, which we lately have shown to be the case (Phys. Rev. Lett. **89**,

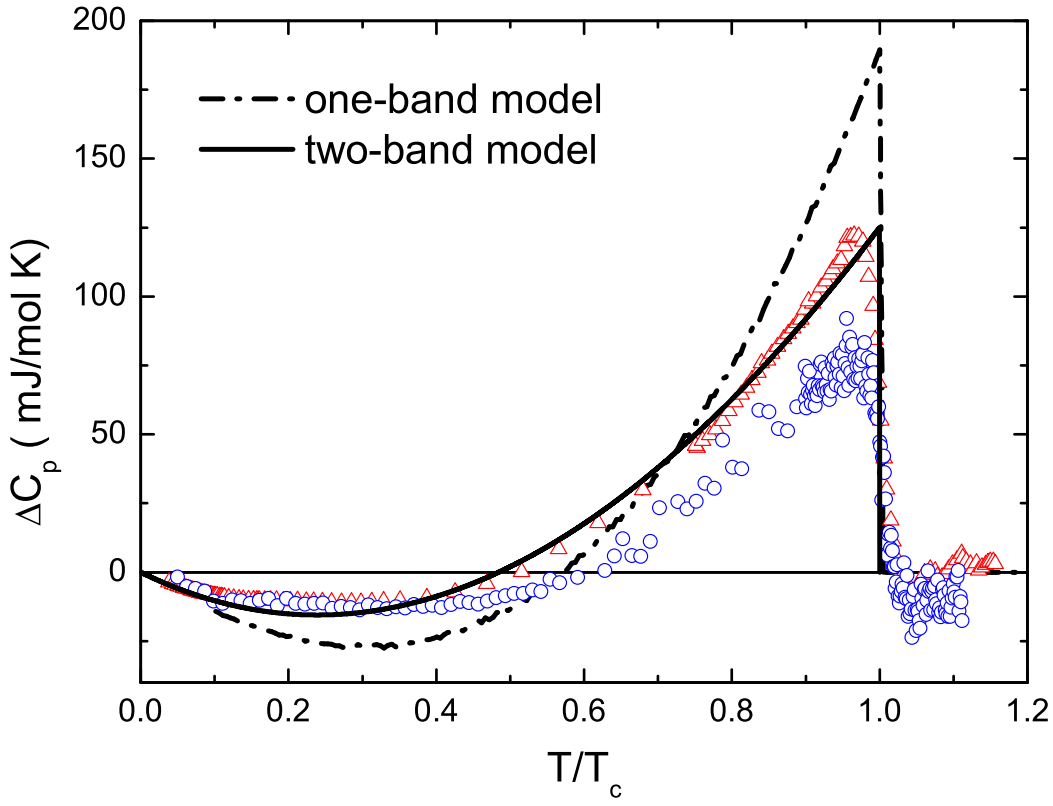

Figure 2: *Experimental data of the heat capacity difference* $\Delta C_p = C_p(0\text{Tesla}) - C_p(9\text{Tesla})$ *measured by us* ($\circ$) *and by Bouquet et al. [Phys. Rev. Lett.* **87**, *047001 (2001)]* ($\triangle$). *The dashed line is the theoretical result of the one-band model and the thick solid line corresponds to the two-band model from the solution of the Eliashberg equations. The two-band model reproduces much better the specific heat jump as well as the low temperature behaviour.*

107002 (2002)).

We therefore recalculated the Eliashberg functions allowing for two different order parameters for the σ and π-electrons. The corresponding Eliashberg functions are shown in Fig.3. As expected the most significant contribution comes from the coupling of the bond-streching phonon modes to the σ-band.

Besides the spectral functions we need the information of the Coulomb matrix element μ_{ij}. With the help of the wavefunctions from our first-principles calculations we can approximately calculate the ratio of the elements of the μ-matrix. The ratio between $\sigma\sigma$, $\pi\pi$ and $\sigma\pi$ were 2.23/2.48/1. This allows one to express μ^*_{ij} by these ratios and one single free parameter which is fixed to get the experimental T_c of 39.4 K from the solution of the Eliashberg equations.

Using our calculated Eliashberg functions on the imaginary (Matsubara) axis together with the above matrix μ^*_{ij} we obtain the gap values $\Delta_\sigma = \lim_{T\to 0} \Delta_\sigma(i\pi T) \simeq 7.1\,\text{meV}$, and $\Delta_\pi \simeq 2.7\,\text{meV}$, which corresponds to $2\Delta_\sigma/k_BT_c$=4.18 and $2\Delta_\pi/k_BT_c$=1.59 and which are in good

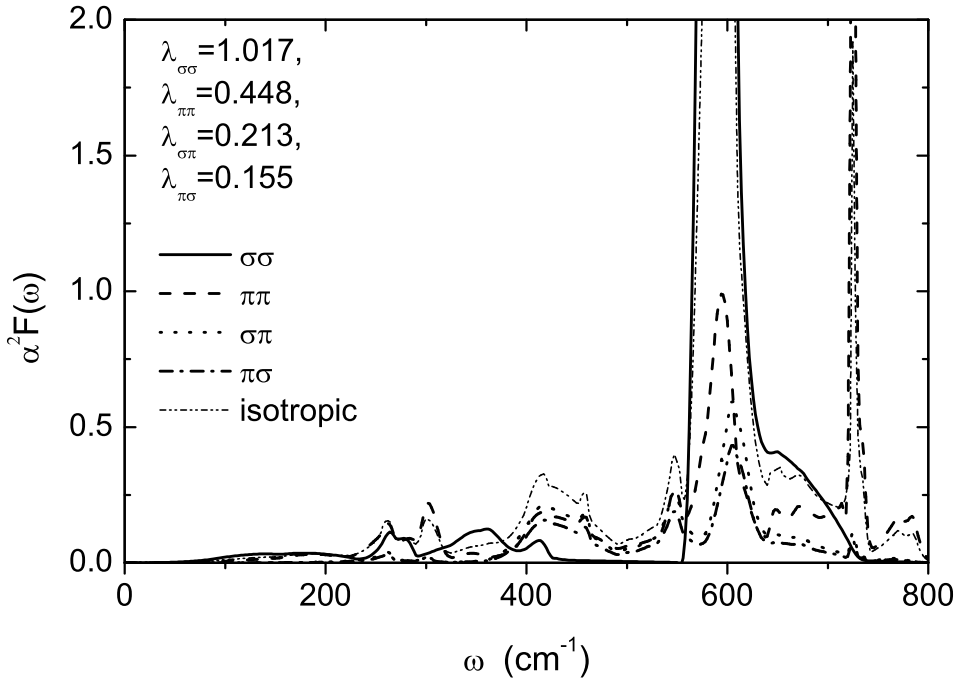

Figure 3: *The four superconducting Eliashberg functions* $\alpha^2 F(\omega)$ *obtained from first-principles calculations for the effective two-band model are compared with the isotropic Eliashberg function for the one-band model. The coupling constant of the isotropic one-band model has a value of* λ_{iso}*=0.87.*

agreement with several experiments.

We solved the two band Eliashberg equations as function of temperature and calculated the difference between the specific heat in the superconducting state and the normal state which is shown in Fig.2. It may be seen that not only the specific heat jump at T_c but also the low temperature behaviour is in much better agreement with experiments than the results of the one-band model.

The multiband model was further confirmed by the agreement with experiments of the calculated Josephson tunneling in MgB_2-based junctions (Phys. Rev. B **65**, 180517 (2002)), the temperature dependence and anisotropy of the magnetic-field penetration depth (Phys. Rev. B **66**, 054524 (2002)), and the calculated de Haas-van Alphen mass renormalization (Phys. Rev. B **65**, 180510 (2002)).